

KINEMATICS AND SINGULARITY ANALYSIS OF A CRRHRRRC PARALLEL SCHÖNFLIES MOTION GENERATOR

Takashi Harada¹, Jorge Angeles²

¹*Department of Mechanical Engineering, Faculty of Science and Engineering,
Kinki University, Higashiosaka, Osaka, Japan*

²*Department of Mechanical Engineering and Center for Intelligent Machines,
McGill University, Montreal, Quebec, Canada*

Email: harada@mech.kindai.ac.jp; angeles@cim.mcgill.ca

ABSTRACT

A novel architecture for a parallel Schönflies motion generator was recently proposed by C.C. Lee, consisting of a CRRHRRRC linkage. The novelty of this architecture lies in a) its simplicity, as it comprises only two limbs, thereby forming a single-loop closed kinematic chain and b) its actuator mechanism, which is based on two-degree-of-freedom cylindrical joints. Moreover, its moving plate is coupled to the two limbs by means of corresponding coaxial H pairs. This paper reports on the kinematics and singularity analysis of this robot, intended for fast pick-and-place operations. A prototype of the robot is currently under development at McGill University's Centre for Intelligent Machines.

Keywords: Schönflies motion generators; kinematics; Jacobian analysis; singularity analysis.

ANALYSES CINÉMATIQUE ET DE SINGULARITÉ D'UN ROBOT PARALLÈLE CRRHRRRC POUR LA PRODUCTION DE MOUVEMENTS DE SCHÖNFLIES

RÉSUMÉ

M. C.C. Lee a proposé récemment une architecture novatrice pour un robot parallèle CRRHRRRC destiné à la production de mouvements de Schönflies. L'aspect novateur de cette architecture porte sur a) sa simplicité, car elle ne comporte que deux membres, ce qui se traduit par une chaîne cinématique à une seule boucle, et b) son mécanisme d'actuation, basé sur des articulations cylindriques, qui comportent deux degrés de liberté. En outre, la plate-forme mobile est couplée aux deux membres par des articulations cinématiques coaxiales du type H. Cette communication fait le point sur la cinématique et l'analyse de singularité du robot qui destiné aux opérations rapides de transfert. Un prototype de ce robot fait l'objet de travaux au *Centre de recherche sur les machines intelligentes* de l'Université McGill.

Mots-clés : Mécanismes pour la production de mouvements de Schönflies ; cinématique ; analyse de la jacobienne ; analyse de singularité.

1. INTRODUCTION

Schönflies motions comprise three translations and one rotation, as seen on the motions of a waiter's tray, occur frequently in pick-and-place operations. Robots for industrial assembly and packaging, capable of these motions are thus termed Schönflies motion generators (SMGs). Current R&D work in connection with SMGs targets fast operations, their performance being measured in the number of test cycles that can be executed by these robots in one second. The record is three cycles per second on an industry-adopted trajectory: 25 mm up from a moving-plate (MP) home pose, followed by a 300-mm horizontal path, down 25 mm and back to the home pose following the same path in the opposite direction. Moreover, during the horizontal segment of the path, the MP is to turn 180° cw in the first half of the cycle, 180° ccw when returning.

Some parallel robots producing Schönflies motion can be cited: The McGill SMG [1], the H4 [2], [3], I4L, I4R, Heli and Par4. Adept Technology's Quattro is the fastest SMG in the market. Quattro is supplied with four limbs that connect the MP with the base plate (BP). In the Quattro and I4L, the rotation is obtained through gear trains, to provide for a rotation amplification [3]. The latter is needed because of the low rotatability of the MP by virtue of the four limbs, which contributes to the complexity of the mechanism. Recently, an alternative architecture was proposed by C.C. Lee [4], which entails coaxial helical (H) joints¹ to achieve the rotation of the MP. H pairs being available off-the-shelf, a coaxial HH subchain can be readily designed for producing a full rotation of the MP. Research on the feasibility of a HH mechanism, along with the kinematics, dynamics, optimum design, prototyping, and control of a SMG with Lee's architecture, dubbed the *Peppermill* because of the resemblance of its MP with a large wooden peppermill, is now underway at McGill University's *Centre for Intelligent Machines*, in collaboration with Japan's Kinki University. In this paper, the kinematic model, position and velocity analysis of the HH mechanism are introduced as a first step of the feasibility study. The singularities of the mechanism are identified.

2. KINEMATIC MODEL OF THE PEPPERMILL

A schematic view of the Peppermill is illustrated in Fig. 1. Two CRR limbs are connected to the MP, that carries a coaxial subchain of H joints. The Peppermill is made up of a single-loop linkage of the CRRHHRRC type. The C joints of the linkage are driven by identical rotational motors in a differential array of ball-screw drives (see Appendix A); the axis of the i th C joint, for $i = 1, 2$, termed here the i th-drive axis, is parallel to the unit vector \mathbf{a}_i . Moreover, d_i and θ_i denote the translational and rotational displacement variables of the i th limb, respectively, with d_i measured in units of length, θ_i in radians. Points O_i denote the intersection of the i th-drive axis with the common normal to the two, which is the z -axis of the base frame.

The fixed origin O of the base frame is set at the midpoint of segment $\overline{O_1O_2}$, as shown in Fig. 1. Unit vectors parallel to the x , y and z axes are defined as \mathbf{i} , \mathbf{j} and \mathbf{k} , respectively. The angle of rotation of the proximal passive R joint is defined as λ_i , while \mathbf{u}_i and \mathbf{v}_i are unit vectors parallel to the axes of the proximal and the distal links of the i th limb, respectively. Furthermore, r_i and l_i denote the lengths of the proximal and the distal links, respectively. The end of the distal link of the i th limb is coupled with the passive R pair of the MP at point P_i . The pose of the MP is given by $\mathbf{c} = [x, y, z]^T$, the position vector of point C , and angle ϕ , as shown in Fig. 1. Angle ϕ , in turn, is measured from a predefined orientation of the axially symmetric MP.

¹In this paper, the standard nomenclature of kinematic chains is used, whereby C, H and R denote, respectively, cylindrical, helical (or screw) and revolute kinematic pairs.

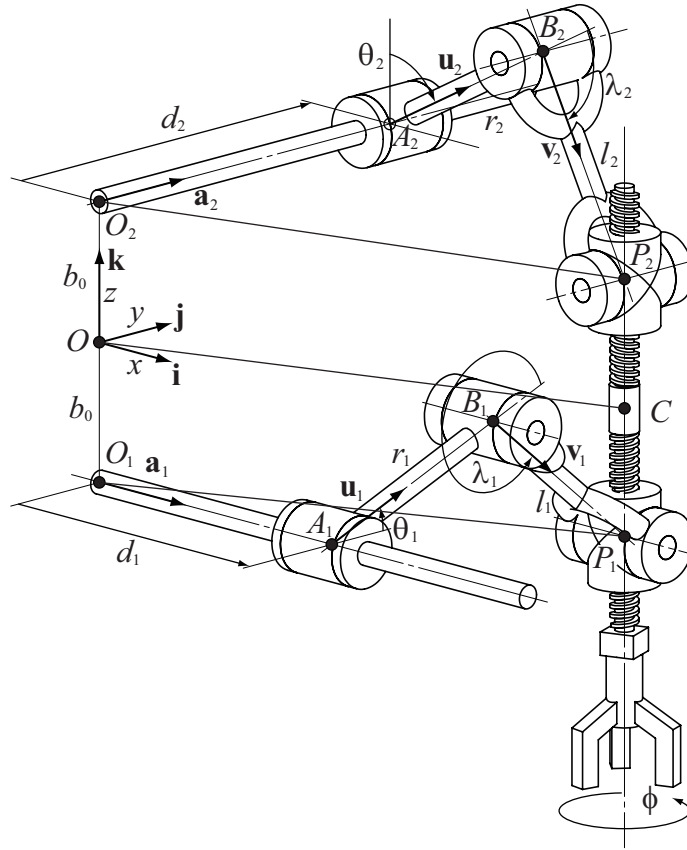


Fig. 1. Schematic view of Lee's SMG

3. DISPLACEMENT ANALYSIS OF THE SMG

3.1. Vector Loop Equations

Vector $\overrightarrow{O_i P_i}$ is described upon following two paths:

$$\mathbf{p}_i = \overrightarrow{O_i P_i} = \overrightarrow{O_i A_i} + \overrightarrow{A_i B_i} + \overrightarrow{B_i P_i} \quad (1)$$

$$\mathbf{p}_i = \overrightarrow{O_i P_i} = \overrightarrow{O_i O} + \overrightarrow{OC} + \overrightarrow{CP_i} \quad (2)$$

the first expression obtained along the i th limb, the second via point C of the MP, the two paths shown in Fig. 1. Therefore, the first expression involves actuator coordinates d_i and θ_i , the second the Cartesian coordinates of the MP, namely, x , y , z and ϕ .

The various vectors appearing in the rightmost-hand side of eq. (1) are readily expressed in terms of actuator variables, namely,

$$\overrightarrow{O_i A_i} = d_i \mathbf{a}_i \quad (3)$$

$$\overrightarrow{O_1 A_1} = d_1 \mathbf{i} \quad (4)$$

$$\overrightarrow{O_2 A_2} = d_2 \mathbf{j} \quad (5)$$

Moreover,

$$\overrightarrow{A_i B_i} = r_i \mathbf{u}_i(\theta_i) \quad (6)$$

where

$$\mathbf{u}_i(\theta_i) = \cos \theta_i \mathbf{x}_i + \sin \theta_i \mathbf{y}_i \quad (7)$$

$$\mathbf{u}_1(\theta_1) = \cos \theta_1 \mathbf{j} + \sin \theta_1 \mathbf{k} \quad (8)$$

$$\mathbf{u}_2(\theta_2) = \cos \theta_2 \mathbf{k} + \sin \theta_2 \mathbf{i} \quad (9)$$

and

$$\overrightarrow{B_i P_i} = l_i \mathbf{v}_i(\theta_i, \lambda_i) \quad (10)$$

where

$$\mathbf{v}_i(\theta_i, \lambda_i) = \cos(\theta_i + \lambda_i) \mathbf{x}_i + \sin(\theta_i + \lambda_i) \mathbf{y}_i \quad (11)$$

$$\mathbf{v}_1(\theta_1, \lambda_1) = \cos(\theta_1 + \lambda_1) \mathbf{j} + \sin(\theta_1 + \lambda_1) \mathbf{k} \quad (12)$$

$$\mathbf{v}_2(\theta_2, \lambda_2) = \cos(\theta_2 + \lambda_2) \mathbf{k} + \sin(\theta_2 + \lambda_2) \mathbf{i} \quad (13)$$

Expressions for vectors in the rightmost-hand side of eq. (2) are given below:

$$\overrightarrow{O_i O} = -\overrightarrow{OO_i} \quad (14)$$

$$\overrightarrow{OO_i} = \mathbf{o}_i = b_0 \mathbf{k} \quad (15)$$

$$\overrightarrow{OO_1} = \mathbf{o}_1 = -b_0 \mathbf{k} \quad (16)$$

$$\overrightarrow{OO_2} = \mathbf{o}_2 = b_0 \mathbf{k} \quad (17)$$

In eqs. (16–17), b_0 is the distance between O and O_i , as shown in Fig. 1. Moreover,

$$\overrightarrow{OC} = \mathbf{c} = \begin{bmatrix} x \\ y \\ z \end{bmatrix} \quad (18)$$

and

$$\overrightarrow{CP_i} = p_i \phi \mathbf{k} \quad (19)$$

$$\overrightarrow{CP_1} = p_1 \phi \mathbf{k} \quad (20)$$

$$\overrightarrow{CP_2} = p_2 \phi \mathbf{k} \quad (21)$$

In eqs. (20–21), p_i is the pitch of the i th H pair.

Upon substituting eqs. (4–21) into eqs. (1) and (2), one obtains two corresponding expressions for the same vector \mathbf{p}_i , namely,

$$\mathbf{p}_i = d_i \mathbf{a}_i + r_i \mathbf{u}_i(\theta_i) + l_i \mathbf{v}_i(\theta_i, \lambda_i) \quad (22)$$

$$\mathbf{p}_i = -b_0 \mathbf{k} + \mathbf{c} + p_i \phi \mathbf{k} \quad (23)$$

Upon equating the right-hand sides of eqs. (1) and (2), thereby closing the loop, one obtains

$$d_i \mathbf{a}_i + r_i \mathbf{u}_i(\theta_i) + l_i \mathbf{v}_i(\theta_i, \lambda_i) = -b_0 \mathbf{k} + \mathbf{c} + p_i \phi \mathbf{k} \quad (24)$$

which is the mechanism loop-closure equation.

3.2. Inverse Displacement Analysis

For the inverse displacement analysis, the actuator-joint variables, d_1 , d_2 , θ_1 and θ_2 , are to be obtained from both the position vector $\mathbf{c} = [x, y, z]^T$ and angle ϕ , which define the pose of the MP.

Upon pre-multiplying the expression \mathbf{p}_i of eq. (22) by \mathbf{a}_i^T , one obtains

$$\mathbf{a}_i^T \mathbf{p}_i = d_i \mathbf{a}_i^T \mathbf{a}_i + r_i \mathbf{a}_i^T \mathbf{u}_i(\theta_i) + l_i \mathbf{a}_i^T \mathbf{v}_i(\theta_i, \lambda_i) = d_i \quad (25)$$

Note that, $\mathbf{a}_i^T \mathbf{a}_i = 1$, and \mathbf{a}_i is perpendicular to both \mathbf{u}_i and \mathbf{v}_i , whence $\mathbf{a}_i^T \mathbf{u}_i = 0$ and $\mathbf{a}_i^T \mathbf{v}_i = 0$.

Furthermore, upon pre-multiplying \mathbf{p}_i of eq. (23) by \mathbf{a}_i^T , for $i = 1, 2$, one obtains,

$$\begin{aligned} \mathbf{a}_1^T \mathbf{p}_1 &= \mathbf{i}^T (b_0 \mathbf{k} + \mathbf{c} + p_1 \phi \mathbf{k}) \\ &= [1 \ 0 \ 0] \left(\begin{bmatrix} 0 \\ 0 \\ b_0 \end{bmatrix} + \begin{bmatrix} x \\ y \\ z \end{bmatrix} + \begin{bmatrix} 0 \\ 0 \\ p_1 \phi \end{bmatrix} \right) = x \end{aligned} \quad (26)$$

$$\begin{aligned} \mathbf{a}_2^T \mathbf{p}_2 &= \mathbf{j}^T (-b_0 \mathbf{k} + \mathbf{c} + p_2 \phi \mathbf{k}) \\ &= [0 \ 1 \ 0] \left(\begin{bmatrix} 0 \\ 0 \\ -b_0 \end{bmatrix} + \begin{bmatrix} x \\ y \\ z \end{bmatrix} + \begin{bmatrix} 0 \\ 0 \\ p_2 \phi \end{bmatrix} \right) = y \end{aligned} \quad (27)$$

From eqs. (25–27), d_1 and d_2 are readily obtained as

$$d_1 = x, \quad d_2 = y \quad (28)$$

Next, angle θ_i of the i th actuated joint is to be derived upon eliminating angle λ_i of the passive joint. From eqs. (22–24), one obtains

$$\mathbf{p}_i - d_i \mathbf{a}_i = r_i \mathbf{u}_i(\theta_i) + l_i \mathbf{v}_i(\theta_i, \lambda_i) \quad (29)$$

Note here that \mathbf{p}_i and $d_i \mathbf{a}_i$ are known. For simplicity, the left-hand side of eq. (29) is defined as \mathbf{q}_i . Equation (29) then leading to

$$l_i \mathbf{v}_i(\theta_i, \lambda_i) = \mathbf{q}_i - r_i \mathbf{u}_i(\theta_i) \quad (30)$$

In order to eliminate the passive joint variables $\mathbf{v}_i(\theta_i, \lambda_i)$, both sides of eq. (30) are premultiplied by their corresponding transpose, whence,

$$l_i^2 \mathbf{v}_i^T \mathbf{v}_i = \mathbf{q}_i^T \mathbf{q}_i - 2r_i \mathbf{q}_i^T \mathbf{u}_i + r_i^2 \mathbf{u}_i^T \mathbf{u}_i$$

or

$$l_i^2 = \mathbf{q}_i^T \mathbf{q}_i - 2r_i \mathbf{q}_i^T \mathbf{u}_i + r_i^2 \quad (31)$$

Hence,

$$2r_i \mathbf{q}_i^T \mathbf{u}_i = \mathbf{q}_i^T \mathbf{q}_i + r_i^2 - l_i^2 \quad (32)$$

Upon substituting eq. (7) into eq. (32), one obtains

$$2r_i \mathbf{q}_i^T (\cos \theta_i \mathbf{x}_i + \sin \theta_i \mathbf{y}_i) = \mathbf{q}_i^T \mathbf{q}_i + r_i^2 - l_i^2$$

where θ_i is obtained from the relation

$$(\mathbf{q}_i^T \mathbf{x}_i) \cos \theta_i + (\mathbf{q}_i^T \mathbf{y}_i) \sin \theta_i = \frac{\mathbf{q}_i^T \mathbf{q}_i + r_i^2 - l_i^2}{2r_i} \quad (33)$$

Furthermore, the unit vector of the distal link \mathbf{v}_i is given from eq. (30) as

$$\mathbf{v}_i = \frac{\mathbf{q}_i - r_i \mathbf{u}_i}{l_i} \quad (34)$$

Equations (28) and the solutions of eq. (33) yield the inverse displacement solutions of the mechanism.

3.3. Forward Displacement Analysis

In this case, the position $\mathbf{c} = [x, y, z]^T$ and the orientation ϕ of the MP are determined from the prescribed actuated-joint variables, d_i and θ_i , for $i = 1, 2$. From eqs. (28), the coordinates x and y of the MP are given *directly* in terms of the actuated-joint variables d_1 and d_2 , which need no further work, i.e.,

$$x = d_1, \quad y = d_2 \quad (35)$$

The loop-closure equations (24) are expressed in vector form as

$$\begin{bmatrix} d_1 \\ 0 \\ 0 \end{bmatrix} + \begin{bmatrix} 0 \\ r_1 \cos \theta_1 \\ r_1 \sin \theta_1 \end{bmatrix} + \begin{bmatrix} 0 \\ l_1 \cos(\theta_1 + \lambda_1) \\ l_1 \sin(\theta_1 + \lambda_1) \end{bmatrix} = \begin{bmatrix} 0 \\ 0 \\ b_0 \end{bmatrix} + \begin{bmatrix} x \\ y \\ z \end{bmatrix} + \begin{bmatrix} 0 \\ 0 \\ p_1 \phi \end{bmatrix} \quad (36)$$

$$\begin{bmatrix} 0 \\ d_2 \\ 0 \end{bmatrix} + \begin{bmatrix} r_2 \sin \theta_2 \\ 0 \\ r_2 \cos \theta_2 \end{bmatrix} + \begin{bmatrix} l_2 \sin(\theta_2 + \lambda_2) \\ 0 \\ l_2 \cos(\theta_2 + \lambda_2) \end{bmatrix} = \begin{bmatrix} 0 \\ 0 \\ -b_0 \end{bmatrix} + \begin{bmatrix} x \\ y \\ z \end{bmatrix} + \begin{bmatrix} 0 \\ 0 \\ p_2 \phi \end{bmatrix} \quad (37)$$

From the first row of eq. (37) and the first of eqs. (35), one obtains

$$d_1 = r_2 \sin \theta_2 + l_2 \sin(\theta_2 + \lambda_2) \quad (38)$$

whence the passive-joint angle λ_2 is derived as

$$\lambda_2 = \arcsin\left(\frac{d_1 - r_2 \sin \theta_2}{l_2}\right) - \theta_2 \quad (39)$$

Likewise, the passive-joint variable λ_1 is derived from the second row of eq. (36) and the second of eqs. (35) as

$$d_2 = r_1 \cos \theta_1 + l_1 \cos(\theta_1 + \lambda_1), \quad \lambda_1 = \arccos\left(\frac{d_2 - r_1 \cos \theta_1}{l_1}\right) - \theta_1 \quad (40)$$

From the third rows of eqs. (36) and (37), moreover,

$$b_0 + z + p_1 \phi = r_1 \sin \theta_1 + l_1 \sin(\theta_1 + \lambda_1) \quad (41a)$$

$$-b_0 + z + p_2 \phi = r_2 \cos \theta_2 + l_2 \cos(\theta_2 + \lambda_2) \quad (41b)$$

The right-hand sides of eqs. (41a & b) are known because λ_1 and λ_2 have already been derived in eqs. (39 & 40), respectively, while z and ϕ are obtained from the relation below:

$$\begin{bmatrix} 1 & p_1 \\ 1 & p_2 \end{bmatrix} \begin{bmatrix} z \\ \phi \end{bmatrix} = \begin{bmatrix} r_1 \sin \theta_1 + l_1 \sin(\theta_1 + \lambda_1) - b_0 \\ r_2 \cos \theta_2 + l_2 \cos(\theta_2 + \lambda_2) + b_0 \end{bmatrix} \quad (42)$$

which can be inverted as long as the coefficient matrix on the left-hand side is non-singular. This is the case as long as $p_1 \neq p_2$, i.e., as long as the pitches of the two H joints of the MP are distinct.

4. JACOBIAN ANALYSIS

4.1. Jacobian Matrix of the SMG

The two Jacobian matrices of the Peppermill are derived by applying the approach based on virtual displacements to the loop closure equation (24), as proposed by Arai [5], thereby deriving

$$\begin{aligned} \delta d_i \mathbf{a}_i + d_i \delta \mathbf{a}_i &+ \delta r_i \mathbf{u}_i(\theta_i) + r_i \delta \mathbf{u}_i(\theta_i) + \delta l_i \mathbf{v}_i + l_i \delta \mathbf{v}_i \\ &= -\delta b_{0i} \mathbf{k} - b_{0i} \delta \mathbf{k} + \delta \mathbf{c} + (\delta p_i \phi + p_i \delta \phi) \mathbf{k} + p_i \phi \delta \mathbf{k} \end{aligned} \quad (43)$$

Further it is recalled that the link lengths r_i and l_i , the pitch p_i of the H joint, and the unit vectors \mathbf{a}_i and \mathbf{k}_i are constant. Hence, the variations undergone by these quantities, as appearing in eq. (43), vanish, eq. (43) thus simplifying to

$$\delta d_i \mathbf{a}_i + r_i \delta \mathbf{u}_i(\theta_i) + l_i \delta \mathbf{v}_i = \delta \mathbf{c} + p_i \delta \phi \mathbf{k} \quad (44)$$

From eq. (7),

$$\begin{aligned} \delta \mathbf{u}_i \theta_i &= \delta(\cos \theta_i \mathbf{x}_i + \sin \theta_i \mathbf{y}_i) \\ &= (-\sin \theta_i \mathbf{x}_i + \cos \theta_i \mathbf{y}_i) \delta \theta = \mathbf{u}_{\theta i} \delta \theta \end{aligned} \quad (45)$$

$$\mathbf{u}_{\theta i} = (-\sin \theta_i \mathbf{x}_i + \cos \theta_i \mathbf{y}_i) \quad (46)$$

Substituting eq. (46) into eq. (44), one obtains,

$$\delta d_i \mathbf{a}_i + r_i \mathbf{u}_{\theta i} \delta \theta_i + l_i \delta \mathbf{v}_i = \delta \mathbf{c} + p_i \delta \phi \mathbf{k} \quad (47)$$

Upon pre-multiplying both sides of eq. (47) by \mathbf{a}_i^T and by \mathbf{v}_i^T , one obtains two additional relations:

$$\delta d_i \mathbf{a}_i^T \mathbf{a}_i + r_i \mathbf{a}_i^T \mathbf{u}_{\theta i} \delta \theta_i + l_i \mathbf{a}_i^T \delta \mathbf{v}_i = \mathbf{a}_i^T \delta \mathbf{c} + p_i \delta \phi \mathbf{a}_i^T \mathbf{k} \quad (48)$$

$$\delta d_i \mathbf{v}_i^T \mathbf{a}_i + r_i \mathbf{v}_i^T \mathbf{u}_{\theta i} \delta \theta_i + l_i \mathbf{v}_i^T \delta \mathbf{v}_i = \mathbf{v}_i^T \delta \mathbf{c} + p_i \delta \phi \mathbf{v}_i^T \mathbf{k} \quad (49)$$

As shown in Fig. 1, the various vectors involved in the foregoing equations obey the relations: $\mathbf{a}_i \perp \mathbf{u}_i$, $\mathbf{a}_i \perp \mathbf{u}_{\theta i}$, $\mathbf{a}_i \perp \mathbf{v}_i$, $\mathbf{a}_i \perp \delta \mathbf{v}_i$ and $\mathbf{a}_i \perp \mathbf{k}$. Therefore, the scalar products of these pairs of vectors vanish. As well, two additional relations are recalled:

$$\mathbf{a}_i^T \mathbf{a}_i = 1, \quad \mathbf{v}_i^T \delta \mathbf{v}_i = 0$$

equations (48) and (49) thus reducing to

$$\delta d_i = \mathbf{a}_i^T \delta \mathbf{c} \quad (50)$$

$$r_i \mathbf{v}_i^T \mathbf{u}_{\theta i} \delta \theta_i = \mathbf{v}_i^T \delta \mathbf{c} + p_i \delta \phi \mathbf{v}_i^T \mathbf{k} \quad (51)$$

with $\delta \mathbf{c}$ representing a small displacement of the position of point C of the MP, of components δx , δy and δz .

Equations (50 & 51) express the relationship between the small displacement $\delta \mathbf{c}$ and the small angle $\delta \phi$ of the MP with the small variations of the actuated-joint variables δd_i and $\delta \theta_i$ of the i th driving unit.

Relationship between the small displacements of the MP and those of the actuated joints are expressed below using Jacobian matrices:

$$\begin{bmatrix} \mathbf{a}_1^T & 0 \\ \mathbf{a}_2^T & 0 \\ \mathbf{v}_1^T & p_1 \mathbf{v}_1^T \mathbf{k} \\ \mathbf{v}_2^T & p_2 \mathbf{v}_2^T \mathbf{k} \end{bmatrix} \begin{bmatrix} \delta x \\ \delta y \\ \delta z \\ \delta \phi \end{bmatrix} = \begin{bmatrix} 1 & 0 & 0 & 0 \\ 0 & 1 & 0 & 0 \\ 0 & 0 & \mathbf{v}_1^T \mathbf{u}_{\theta 1} & 0 \\ 0 & 0 & 0 & \mathbf{v}_2^T \mathbf{u}_{\theta 2} \end{bmatrix} \begin{bmatrix} \delta d_1 \\ \delta d_2 \\ r_1 \delta \theta_1 \\ r_2 \delta \theta_2 \end{bmatrix} \quad (52)$$

The unit vectors \mathbf{v}_i and $\mathbf{u}_{\theta i}$ are represented componentwise as

$$\mathbf{v}_1 = \begin{bmatrix} 0 \\ v_{1y} \\ v_{1z} \end{bmatrix}, \quad \mathbf{v}_2 = \begin{bmatrix} v_{2x} \\ 0 \\ v_{2z} \end{bmatrix} \quad (53)$$

$$\mathbf{u}_{\theta 1} = \begin{bmatrix} 0 \\ u_{\theta 1y} \\ u_{\theta 1z} \end{bmatrix}, \mathbf{u}_{\theta 2} = \begin{bmatrix} u_{\theta 2z} \\ 0 \\ u_{\theta 2z} \end{bmatrix} \quad (54)$$

Upon substitution of the foregoing vectors into eq. (52), one obtains

$$\begin{bmatrix} 1 & 0 & 0 & 0 \\ 0 & 1 & 0 & 0 \\ 0 & v_{1y} & v_{1z} & p_1 v_{1z} \\ v_{2x} & 0 & v_{2z} & p_2 v_{2z} \end{bmatrix} \begin{bmatrix} \delta x \\ \delta y \\ \delta z \\ \delta \phi \end{bmatrix} = \begin{bmatrix} 1 & 0 & 0 & 0 \\ 0 & 1 & 0 & 0 \\ 0 & 0 & \mathbf{v}_1^T \mathbf{u}_{\theta 1} & 0 \\ 0 & 0 & 0 & \mathbf{v}_2^T \mathbf{u}_{\theta 2} \end{bmatrix} \begin{bmatrix} \delta d_1 \\ \delta d_2 \\ r_1 \delta \theta_1 \\ r_2 \delta \theta_2 \end{bmatrix} \quad (55)$$

or, in compact form,

$$\mathbf{A} \delta \mathbf{x} = \mathbf{B} \delta \theta \quad (56)$$

where \mathbf{A} and \mathbf{B} are the two Jacobian matrices of the Peppermill, namely,

$$\mathbf{A} = \begin{bmatrix} 1 & 0 & 0 & 0 \\ 0 & 1 & 0 & 0 \\ 0 & v_{1y} & v_{1z} & p_1 v_{1z} \\ v_{2x} & 0 & v_{2z} & p_2 v_{2z} \end{bmatrix} \quad (57)$$

$$\mathbf{B} = \begin{bmatrix} 1 & 0 & 0 & 0 \\ 0 & 1 & 0 & 0 \\ 0 & 0 & \mathbf{v}_1^T \mathbf{u}_{\theta 1} & 0 \\ 0 & 0 & 0 & \mathbf{v}_2^T \mathbf{u}_{\theta 2} \end{bmatrix} \quad (58)$$

4.2. The Singularity of the First Kind

The singularity of the first kind [6], which is also referred as the inverse-kinematics singularity [7], occurs when the Jacobian matrix \mathbf{B} of eq. (55) is singular, i.e., when

$$\det(\mathbf{B}) = (\mathbf{v}_1^T \mathbf{u}_{\theta 1})(\mathbf{v}_2^T \mathbf{u}_{\theta 2}) = 0 \quad (59)$$

Geometrically, this singularity occurs when $\mathbf{v}_1 \perp \mathbf{u}_{\theta 1}$ or $\mathbf{v}_2 \perp \mathbf{u}_{\theta 2}$, i.e., when the unit vector \mathbf{v}_i of the proximal link and the unit vector \mathbf{u}_i of the distal link are parallel in at least one driving unit. Figure 2 illustrates a posture with the singularity of the first kind.

4.3. The Singularity of the Second Kind

The singularity of the second kind [6], which is also referred as the direct-kinematics singularity, occurs when the Jacobian matrix \mathbf{A} of eq. (57) becomes singular. The singularity of matrix \mathbf{A} , is readily established by virtue of the block structure of the matrix, namely,

$$\begin{aligned} \det(\mathbf{A}) &= \det \left(\left[\begin{array}{cc|cc} 1 & 0 & 0 & 0 \\ 0 & 1 & 0 & 0 \\ \hline 0 & v_{1y} & v_{1z} & p_1 v_{1z} \\ v_{2x} & 0 & v_{2z} & p_2 v_{2z} \end{array} \right] \right) \\ &= \det \left(\begin{bmatrix} 1 & 0 \\ 0 & 1 \end{bmatrix} \right) \det \left(\begin{bmatrix} v_{1z} & p_1 v_{1z} \\ v_{2z} & p_2 v_{2z} \end{bmatrix} \right) \\ &= v_{1z} v_{2z} (p_2 - p_1) = 0 \end{aligned} \quad (60)$$

If $v_{1z} = 0$, or $v_{2z} = 0$, or $p_2 - p_1 = 0$, then matrix \mathbf{A} becomes singular. Geometrically, these conditions occur when

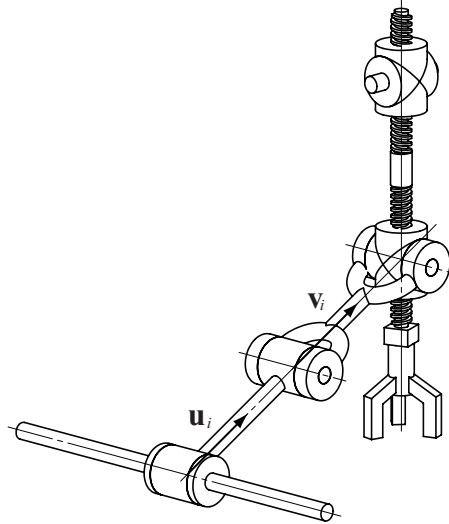


Fig. 2. A robot posture with a singularity of the first kind

1. The unit vector of the distal link of at least one limb lies in the xy plane, i.e., when the unit vector the distal link of at least one limb is normal to the z -axis, and
2. The pitch of the upper H pair equals that of its lower counterpart.

Condition 2 can be readily avoided by choosing the pitches of the H pairs distinct. Even better, we chose the pitches of identical absolute values but of opposite signs, i.e., we chose these two pitches identical, but of opposite hands. Figure 3 illustrates a posture with a singularity of the second kind.

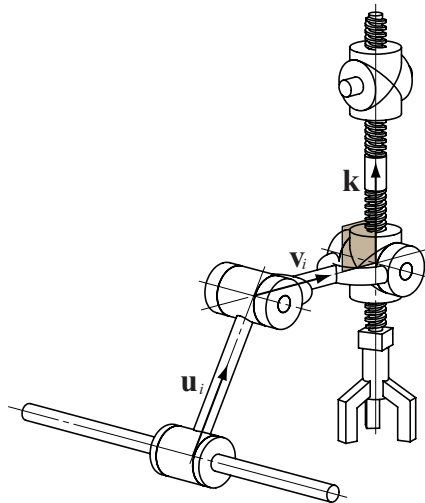


Fig. 3. A robot posture with a singularity of the second kind

4.4. The Singularity of the Third Kind

The singularity of the third kind [6], which is also referred as the complex-kinematics singularity, occurs when the the two Jacobian matrices **A** and **B** become singular. This singularity is of a different kind, as not every robot admits it. Indeed, this singularity depends on the robot architecture. Given the symmetries with

which the Peppermill was designed, this robot admits the singularity of the third kind, as illustrated in Fig. 4.

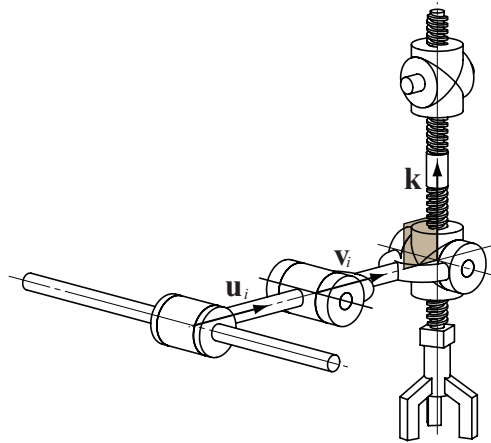


Fig. 4. A robot posture with a singularity of the third kind

5. CONCLUSIONS

The position analysis and Jacobian analyses of a CRRHRRRC Schönflies motion generator (SMG), dubbed here the Peppermill, were discussed here. Vector-loop analysis is applied to derive the position relations of the mechanism. Inverse- and direct-kinematics relations were derived. The two Jacobian matrices were also derived by means of the vector loop equations as applied to virtual displacements. The postures at which the Peppermill finds itself at each of the singularities of the three kinds were identified and illustrated with figures.

ACKNOWLEDGEMENTS

The technical support provided by Damien Trézières, a research trainé from ICAM, in Toulouse, France, is dutifully acknowledged. The first author would like to acknowledge the financial support received from MEXT-supported program for the strategic Research Foundation to Private Universities, 2012-2014. The second author would like to acknowledge the financial support received from NSERC through a Discovery Grant and from McGill University via a James McGill Professorship.

REFERENCES

1. Gauthier, J.F., Angeles, J., Nogleby, S.B. and Morozov, A. "The kinetostatic conditioning of two-limb schönflies motion generators." *Transactions ASME, Journal of Mechanisms and Robotics*, Vol. 1, pp. 011010–1–12, 2009.
2. Pierrot, F. and Company, O. "H4: A new family of 4-dof parallel robots." In "Proceedings of the IEEE/ASME International Conference on Advanced Intelligent Mechatronics," .
3. Company, O., Pierrot, F., Krut, S. and Nabat, V. "Simplified dynamic modelling and improvement of a four-degree-of-freedom pick-and-place manipulator with articulated moving platform." In "Proceedings of the Institution of Mechanical Engineers, Part I:Journal of Systems and Control Engineering," pp. 13–26, 2009.
4. Lee, C.C. and Lee, P.C. "Isoconstrained mechanisms for fast pick-and-place manipulation." in *Lou, Y. and Li, Z. (editors), Geometric Methods in Robotics and Mechanism Research, Lambert Academic Publishing, Saarbrücken, Germany*, pp. 85–99, 2010.
5. Arai, T. "Analysis and sythesis of a parallel link manipulator based on its statics (in japanese)." *Journal of the Robotic Society of Japonon*, Vol. 10, No. 4, pp. 526–533, 1992.

6. Gosselin, C. and Angeles, J. "Singularity analysis of closed-loop kinematic chains." *IEEE Transactions on Robotics and Automation*, Vol. 8, No. 3, pp. 281–290, 1990.
7. Tsai, L.W. *Robot Analysis: The Mechanics of Serial and Parallel Manipulators*. 1 ed.. Wiley-Interscience, 1998.

APPENDIX

Appendix A Conceptual Design of the Cylindrical Joints

Figure A.1 illustrates conceptual design of the cylindrical joint which are driven by identical rotational motors in a differential array of helical-screw drives.

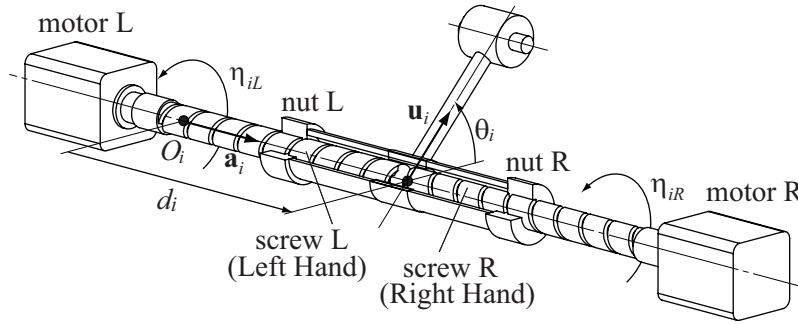


Fig. A.1. Conceptual design of the cylindrical joint

Relationships between displacement of the cylindrical joint, d_i and θ_i , and angles of motors, η_{iL} and η_{iR} , are given as follows:

$$p_{iL}(\eta_{iL} - \theta_i) = d_i \quad (\text{A.1})$$

$$p_{iR}(\eta_{iR} - \theta_i) = d_i \quad (\text{A.2})$$

where $p_{iL} > 0$ and $p_{iR} < 0$ represent the pitches of the Left Hand screw and Right Hand screw, respectively. For simplicity, $i(= 1, 2)$, which represents the number of cylindrical joint, will be dropped from equations after here. In order to simplify the mechanical design and control system of the cylindrical joints, we applied a symmetrical design. Pitches of the screws are expressed by common pitch $p_c (> 0)$ as,

$$p_L = p_c \quad (\text{A.3})$$

$$p_R = -p_c \quad (\text{A.4})$$

From eqs. (A.1–A.4), relationships between displacement of the cylindrical joint, d and θ , and angles of motors, η_L and η_R , in the symmetrical design are simply expressed by a linear equation using matrices as,

$$\begin{bmatrix} p_c & 0 \\ 0 & -p_c \end{bmatrix} \begin{bmatrix} \eta_L \\ \eta_R \end{bmatrix} = \begin{bmatrix} 1 & p_c \\ 1 & -p_c \end{bmatrix} \begin{bmatrix} d \\ \theta \end{bmatrix} \quad (\text{A.5})$$

Inverse displacement analysis which gives the angles of motors, η_L and η_R , from the cylindrical joint valuables, d and θ , is given as,

$$\begin{bmatrix} \eta_L \\ \eta_R \end{bmatrix} = \begin{bmatrix} p_c & 0 \\ 0 & -p_c \end{bmatrix}^{-1} \begin{bmatrix} 1 & p_c \\ 1 & -p_c \end{bmatrix} \begin{bmatrix} d \\ \theta \end{bmatrix} = \begin{bmatrix} \frac{1}{p_c} & 1 \\ -\frac{1}{p_c} & 1 \end{bmatrix} \begin{bmatrix} d \\ \theta \end{bmatrix} \quad (\text{A.6})$$

In the same way, forward displacement analysis is given as,

$$\begin{bmatrix} d \\ \theta \end{bmatrix} = \begin{bmatrix} 1 & p_c \\ 1 & -p_c \end{bmatrix}^{-1} \begin{bmatrix} p_c & 0 \\ 0 & -p_c \end{bmatrix} \begin{bmatrix} \eta_L \\ \eta_R \end{bmatrix} = \begin{bmatrix} \frac{p_c}{2} & -\frac{p_c}{2} \\ \frac{1}{2} & \frac{1}{2} \end{bmatrix} \begin{bmatrix} \eta_L \\ \eta_R \end{bmatrix} \quad (\text{A.7})$$

Jacobian analysis of the cylindrical joint is given by differentiating eq. (A.7) with respect to time as follows:

$$\begin{bmatrix} \dot{d} \\ \dot{\theta} \end{bmatrix} = \begin{bmatrix} \frac{p_c}{2} & -\frac{p_c}{2} \\ \frac{1}{2} & \frac{1}{2} \end{bmatrix} \begin{bmatrix} \dot{\eta}_L \\ \dot{\eta}_R \end{bmatrix} = \mathbf{J}_c \begin{bmatrix} \dot{\eta}_L \\ \dot{\eta}_R \end{bmatrix} \quad (\text{A.8})$$